

Research Paper

Cite this article: Han L, Chen J, Zhang W (2020). Compact UWB monopole antenna with reconfigurable band-notch characteristics. *International Journal of Microwave and Wireless Technologies* **12**, 252–258. <https://doi.org/10.1017/S1759078719001296>

Received: 10 April 2019
Revised: 3 September 2019
Accepted: 7 September 2019
First published online: 4 October 2019


Keywords:

Band-notch; monopole; reconfigurable; ultra-wideband

Author for correspondence:

Liping Han, E-mail: hlp@sxu.edu.cn

Compact UWB monopole antenna with reconfigurable band-notch characteristics

Liping Han , Jing Chen and Wenmei Zhang

School of Physics and Electronic Engineering, Shanxi University, Shanxi 030006, China

Abstract

A compact ultra-wideband (UWB) monopole antenna with reconfigurable band-notch characteristics is demonstrated in this paper. It is comprised of a modified rectangular patch and a defected ground plane. The band-notch property in the WiMAX and WLAN bands is achieved by etching an open-ended slot on the radiating patch and an inverted U-shaped slot on the ground plane, respectively. To obtain the reconfigurable band-notch performance, two PIN diodes are inserted in the slots, and then the notch-band can be switched by changing the states of the PIN diodes. The antenna has a compact size of $0.47 \lambda_1 \times 0.27 \lambda_1$. The simulated and measured results indicate that the antenna can operate at a UWB mode, two single band-notch modes, and a dual band-notch mode. Moreover, stable radiation patterns are obtained.

Introduction

Since the Federal Communications Commission (FCC) released the spectrum from 3.1 to 10.6 GHz for commercial applications, ultra-wideband (UWB) technology has attracted considerable attention due to its low cost, low power consumption, and high data rate. Also, many narrowband systems share their frequency bands with the designated UWB spectrum, such as the WiMAX band (3.4–3.69 GHz), WLAN band (5.15–5.35 GHz, 5.725–5.825 GHz) and ITU band (8.025–8.4 GHz). Therefore, in order to reduce the electromagnetic interference between the narrowband and UWB systems, it is desirable to use UWB antennas with band-notch characteristic. The conventional method for band-notch design is etching different type of slots on the patch or the ground plane, e.g. *L*- and *E*-shaped slot [1], *C*-shaped slot [2], and *U*-shaped and split-ring slot [3], etc. Another approach of band-reject design is loading various parasitic elements, such as modified capacitance loaded loop resonators near the feed line [4], rotated *C*-shaped conductor backed plane under the patch [5], and electromagnetic band-gap (EBG) structure on the CPW line [6].

However, the aforementioned antennas are used for rejecting fixed bands. When there is no interference, the associated notch-band is permanent. In order to effectively utilize the UWB spectrum and improve the performance of the UWB system, it is necessary to design UWB antennas with reconfigurable band-notch performance. The reconfigurability of the notch-band is usually realized by using radio frequency switches, such as PIN diodes and varactor. In the past decades, some UWB antennas with reconfigurable band-notch characteristics have been reported [7–13]. In [9], the reconfigurability of notch-band is obtained by controlling the states of PIN diodes embedded into the inverted *F*-shaped parasitic element and the rectangular split-ring resonator. In [11], the tunable notch is achieved by loading a varactor diode inside a π -shaped slot on the patch. In addition, antennas with reconfigurable band-notch characteristics are presented using optically controlled microwave switches integrated into the folded slot or the complementary split-ring resonator [12, 13].

The main contribution of this work is to demonstrate a miniaturized UWB monopole antenna with reconfigurable band-notch performance. Compared to the antennas with reconfigurable single band-notch property [7, 11, 12], the proposed antenna has single and dual band-notch functions. Moreover, the size of the antenna in this work is the smallest among the reconfigurable single and dual band-notch antennas [8–10, 13]. To produce the band-notch property in the WiMAX and WLAN bands, an open-ended slot and an inverted U-shaped slot are etched on the patch and ground plane, respectively. The reconfigurable band-notch characteristics are obtained by changing the state of the PIN diodes inserted in the slots. The experimental results show that the antenna can switch between a UWB mode, two single band-notch modes, and a dual band-notch mode. Also, good radiation patterns are achieved.

UWB monopole antenna

Figure 1 illustrates the geometry of the UWB monopole antenna. It is fabricated on an inexpensive FR4 substrate with a dielectric constant of 4.4, a loss tangent of 0.02, and a thickness of

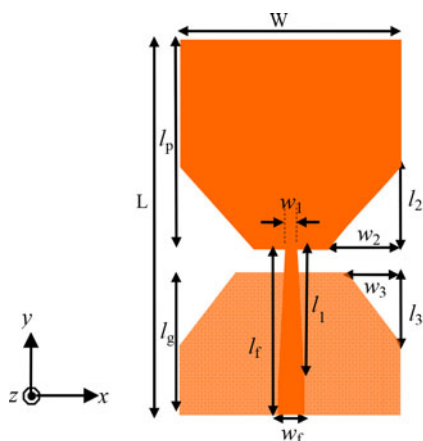


Fig. 1. Geometry of UWB monopole antenna.

0.8 mm. The modified rectangular patch along with the tapered feed-line is printed on the top side of the substrate, and the defected ground plane is printed on the bottom side. The shape of the radiating patch and the ground plane is modified to obtain good impedance matching over the entire UWB frequency range. The antenna is simulated with Ansoft HFSS, and the optimal dimensions are as follows: $L = 31$ mm, $W = 18$ mm, $l_p = 17.5$ mm, $l_g = 12$ mm, $l_f = 13.5$ mm, $w_f = 1.5$ mm, $l_1 = 11$ mm, $w_1 = 0.4$ mm, $l_2 = 7$ mm, $w_2 = 6$ mm, $l_3 = 6$ mm, and $w_3 = 4$ mm, respectively.

To illustrate the good impedance matching of the UWB antenna, Fig. 2 shows the steps of the antenna. The VSWR characteristics for an ordinary rectangular patch (Fig. 2(a)), modified patch (Fig. 2(b)), and the proposed antenna (Fig. 2(c)) are compared in Fig. 3. Compared with the ordinary patch antenna, the impedance bandwidth of the modified patch antenna is significantly improved. Also, the bandwidth can be further enhanced by introducing the self-complementary structure [14,15], as shown in Fig. 2(c).

UWB monopole antenna with reconfigurable band-notch characteristics

Figure 4 shows the geometry of the proposed UWB antenna with reconfigurable band-notch performance. An open-ended slot is etched on the radiating patch to produce the notch-band in the WiMAX band, and an inverted U-shaped slot is embedded on the ground plane to generate the notch-band in the WLAN band. Two PIN diodes (D_1 and D_2) are inserted in the open-ended and inverted U-shaped slots to achieve the reconfigurable band-notch property. Two small C-shaped slots (marked as dark gray) with a width of 0.3 mm are introduced for biasing

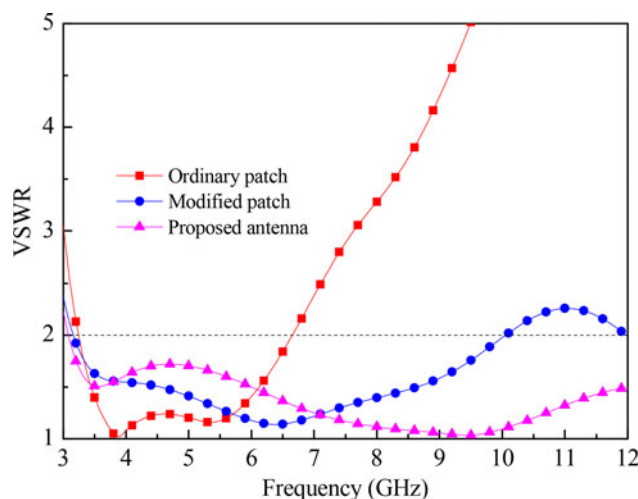


Fig. 3. Simulated VSWR curves for antennas in Fig. 2.

circuits. Three 10 pF capacitors are mounted on the small slots to block the dc passing to the RF source, and one 51 nH inductor is used to isolate the RF signals. To meet the requirements of $VSWR < 2$ within the pass bands of the antenna, a parametric study is performed. The optimal parameters of the band-notch slots are: $l_4 = 11.7$ mm, $l_5 = 1.5$ mm, $l_6 = 3.3$ mm, $l_7 = 0.65$ mm, $l_8 = 1.7$ mm, $l_{g1} = 3$ mm, $l_{g2} = 1.5$ mm, $l_{b1} = 2.1$ mm, $l_{b2} = 2.4$ mm, $l_{b3} = 7.4$ mm, $l_{b4} = 2.4$ mm, and $l_{b5} = 4.1$ mm. The width of the open-ended and inverted U-shaped slots is 0.8 and 0.5 mm, respectively. The dimensions of the feed line, radiating patch, and the ground are the same as those of the antenna in Fig. 1. The BAR50-02V diodes are selected as the switches. According to the datasheet of BAR50-02V, it is modeled by a resistance of 3Ω for ON state and a parallel circuit with a capacitance of 0.15 pF and a resistance of 5 k Ω for OFF state. Table 1. summarizes the operate modes of the antenna. The simulated VSWR characteristics of the antenna are depicted in Fig. 5. It is observed that the antenna can switch between a UWB mode, two single band-notch modes, and a dual band-notch mode. In mode 1 (D_1 and D_2 ON), the antenna provides an impedance bandwidth from 3.1 to 12 GHz. In modes 2 (D_1 OFF and D_2 ON) and 3 (D_1 ON and D_2 OFF), single band-notch property at 3.3–3.7 and 4.9–6.3 GHz is achieved, respectively. In mode 4 (D_1 and D_2 OFF), the antenna exhibits dual band-notch performance at 3.3–3.7 and 5.1–6.5 GHz.

To illustrate the reconfigurable band-notch performance of the antenna, the surface current distributions are studied. Figure 6 plots the simulated current distributions in the dual band-notch

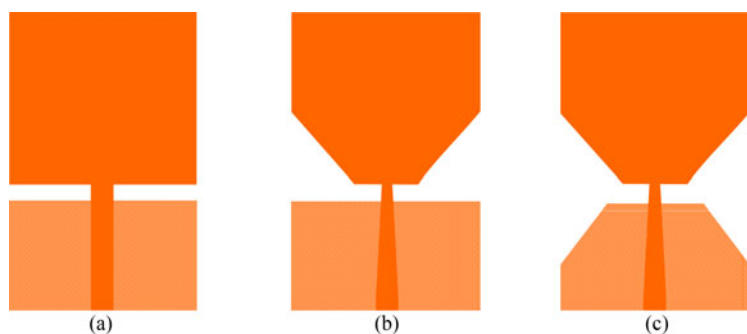


Fig. 2. Steps of bandwidth improvement of the antenna, (a) antenna with ordinary rectangular patch; (b) antenna with modified rectangular patch; (c) proposed antenna.

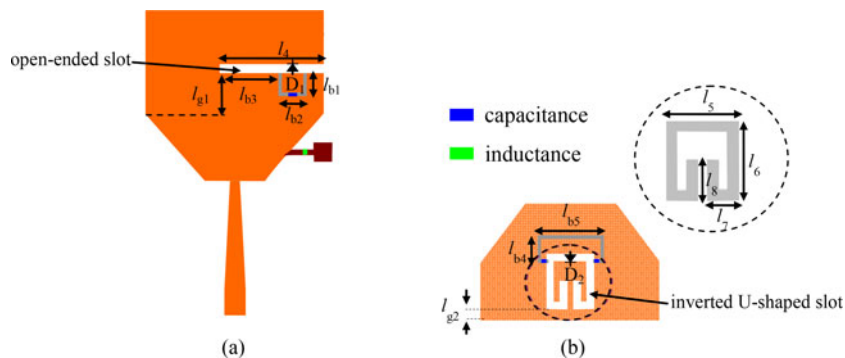


Fig. 4. Geometry of UWB antenna with reconfigurable band-notch characteristics, (a) top view; (b) bottom view (black-diodes, dark gray-biasing slots, blue-block capacitors, green-block inductors, brown-biasing lines).

Table 1. Operate modes of the antenna

Diodes	D_1	D_2	Notch-band (GHz)
Mode 1	ON	ON	-
Mode 2	OFF	ON	3.3–3.7
Mode 3	ON	OFF	4.9–6.3
Mode 4	OFF	OFF	3.3–3.7/5.1–6.5

mode. The current distributions at passband frequencies (4 and 7 GHz) are plotted in Figs 6(a) and 6(b), while the current distributions at the notch frequencies (3.5 and 5.5 GHz) are depicted in Figs 6(c) and 6(d), respectively. As shown in Figs 6(a) and 6(b), it is observed that most currents pass through to the patch and effective radiation can be produced. That is to say there is no attenuation at the passband frequencies. From Fig. 6(c), it is obvious that the currents at 3.5 GHz mainly concentrate on the open-ended slot and change their direction along the edges of the slot. Therefore, powers are reflected back and the notch property at the first notch frequency is achieved. Similarly, the currents at 5.5 GHz are dominant around the inverted U-shaped slot and in opposite

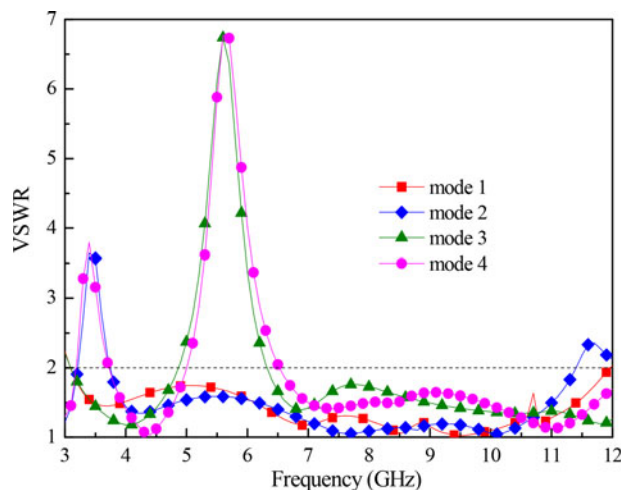


Fig. 5. Simulated VSWR characteristics of the antenna.

direction along the interior and exterior edges of the slot, as illustrated in Fig. 6(d). The radiation field is canceled out and then high attenuation at the second notch frequency is achieved.

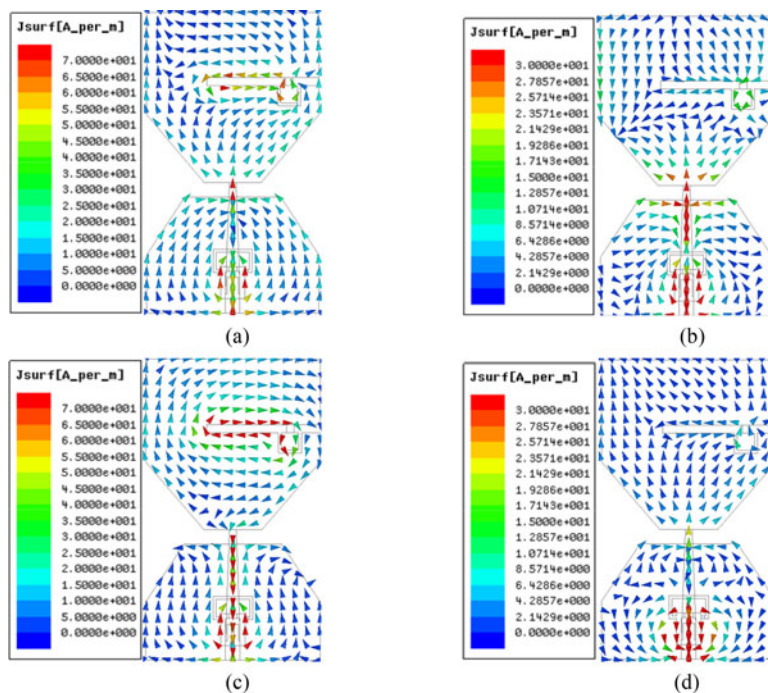


Fig. 6. Simulated surface current distributions in mode 4, (a) at 4 GHz; (b) at 7 GHz; (c) at 3.5 GHz; (d) at 5.5 GHz.

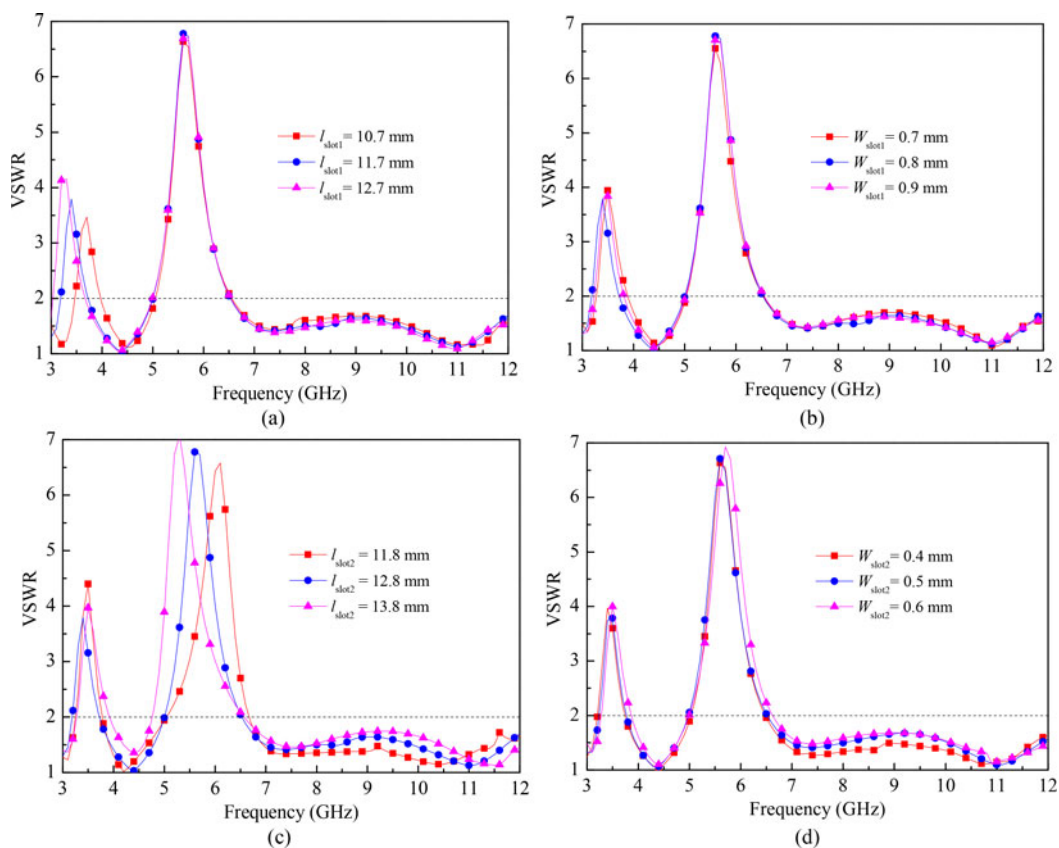


Fig. 7. VSWR characteristics for different slot size, (a) l_{slot1} ; (b) w_{slot1} ; (c) l_{slot2} ; (d) w_{slot2} .

The effect of the slots on the performance of the antenna is also investigated. Figure 7 shows the VSWR characteristics in the dual band-notch mode for different slot size. Let l_{slot1} and l_{slot2} denote the length of the open-ended and inverted U-shaped slots, w_{slot1} and w_{slot2} denote the width of the open-ended and inverted U-shaped slots. As shown in Fig. 7(a), it is observed that when l_{slot1} (l_4) increases, the center frequency of the first notch-band decreases, while that of the second notch-band remains unchanged. From Fig. 7(b), it is found that the center frequency of the notch-bands slightly changes with the increasing w_{slot1} . Similarly, the center frequency of the second notch-band is sensitive to l_{slot2} ($l_5 + 2 \times l_6 + 2 \times l_7 + 2 \times l_8$) and insensitive to w_{slot2} , as illustrated in Figs 7(c) and 7(d). In other words, the notch-band is mainly determined by the length of the band-notch slots. The length of the open-ended slot and inverted U-shaped slot is approximately $\lambda_1/4$ and $\lambda_2/2$ (λ_1 and

λ_2 are the guided wavelength at the center frequency of two notch-bands), respectively. To realize the desired notch-band in the WiMAX and WLAN bands, l_{slot1} and l_{slot2} are selected to be 11.7 and 12.8 mm.

Experimental results

To demonstrate the validity of the proposed design, a prototype of the antenna is fabricated and measured. Figure 8 shows the photo of the fabricated antenna. The VSWR characteristics are measured by an Agilent N5230A vector network analyzer, and the radiation patterns are measured with an SZ-VL antenna automatic test system. The results are shown in Figs 9–11.

Figure 9 shows the simulated and measured VSWR characteristics of the antenna. It can be seen that the antenna can switch among a UWB mode, two single band-notch modes and a dual band-notch mode. A basic agreement between the simulation and measurement results is obtained. In the UWB state, the measured bandwidth for $VSWR < 2$ is 3.07–12 GHz. In the single and dual band-notch modes, the measured notch bandwidth is 3.32–3.83, 5.15–6.94, and 3.17–3.79/5.14–6.82 GHz, respectively. The discrepancy between the simulated and measured ones is mainly caused by the parasitic effects of packaged diodes, the accuracy of the dielectric constant of the material used and the fabrication error.

Figure 10 plots the simulated and measured radiation patterns in the dual band-notch mode. It is observed that the antenna displays bidirectional radiation patterns in the E-plane (yz-plane) and omnidirectional radiation patterns in the H-plane (xz-plane). Table 2 lists the antenna parameters of the radiation patterns. The measured peak gain for the UWB

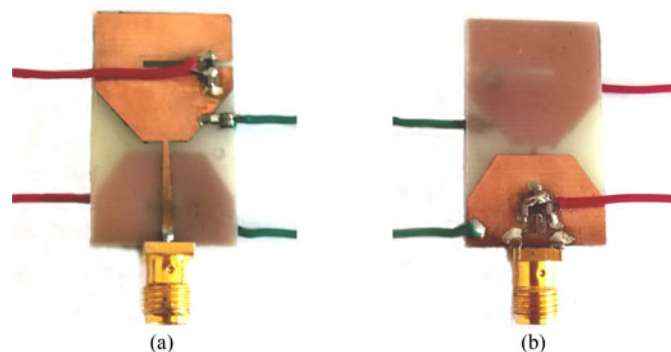


Fig. 8. Photo of the antenna, (a) top view; (b) bottom view.

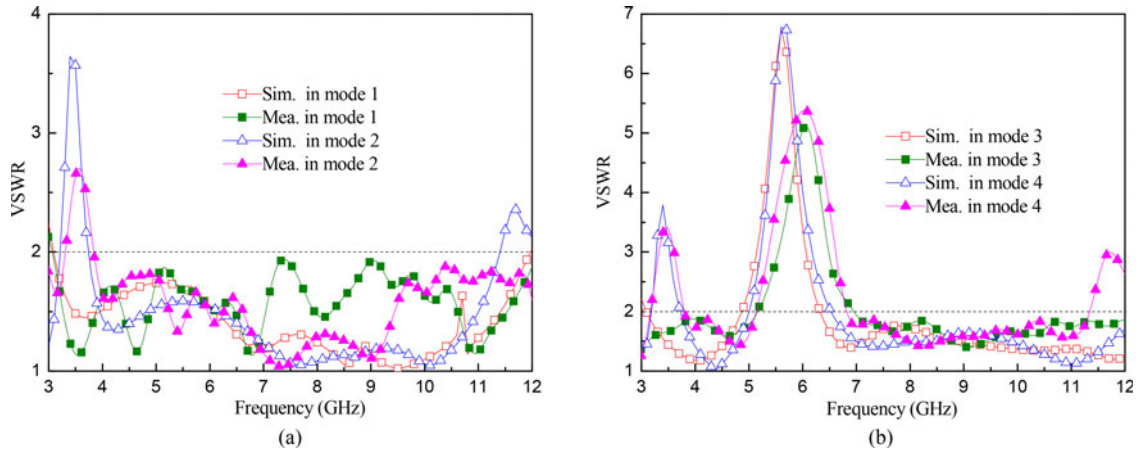


Fig. 9. Simulated and measured VSWR characteristics, (a) in modes 1 and 2; (b) in modes 3 and 4.

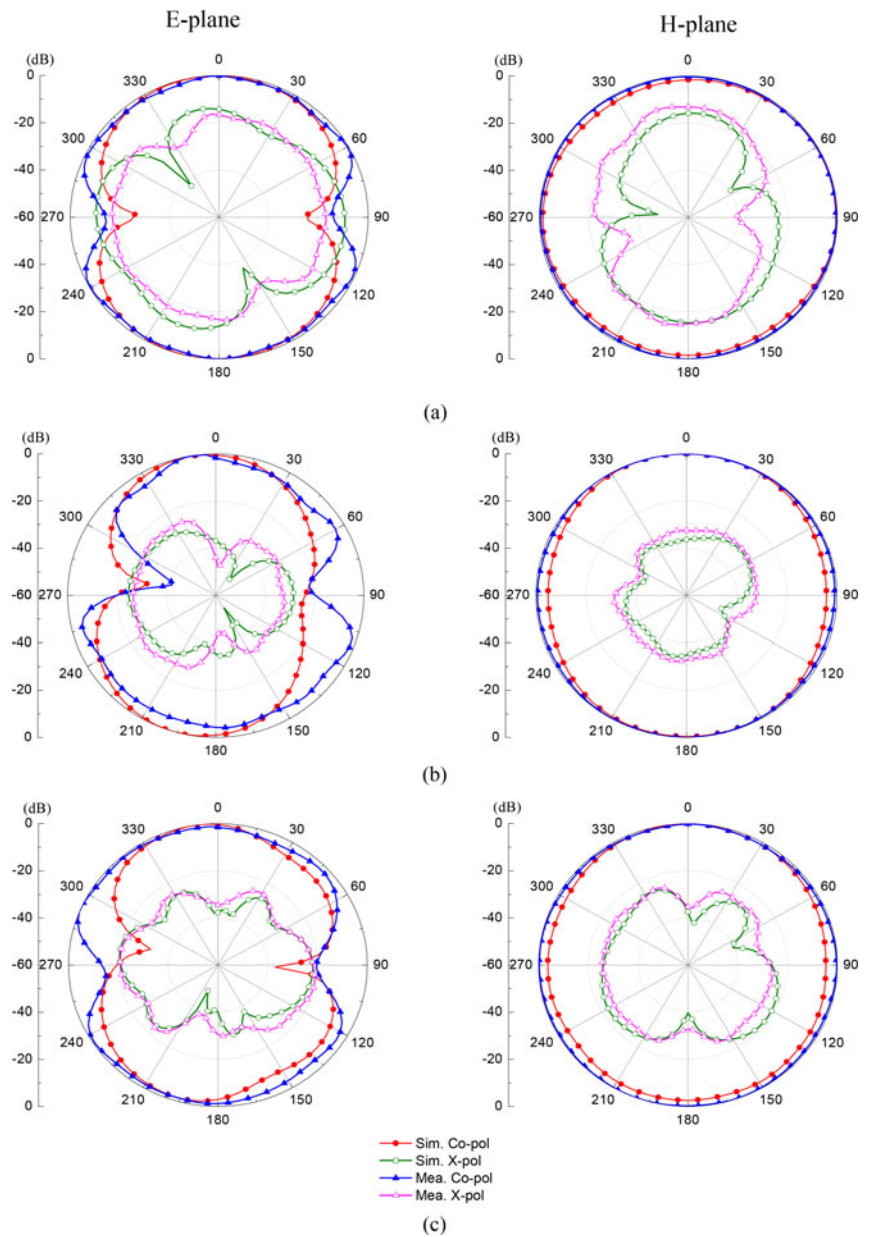


Fig. 10. Simulated and measured radiation patterns, (a) at 4 GHz; (b) at 7 GHz; (c) at 9 GHz.

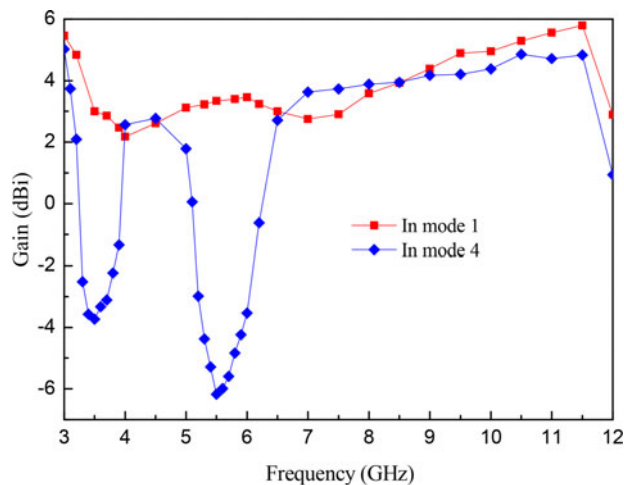


Fig. 11. Measured peak gain in modes 1 and 4.

Table 2. Antenna parameters of radiation patterns in dual band-notch mode

Frequency	E-plane	H-plane	Max x-polar level of E-plane	Max. x-polar level of H-plane
4 GHz	8-shaped	Omnidirectional	-16 dB	-13 dB
7 GHz	8-shaped	Omnidirectional	-25 dB	-30 dB
9 GHz	8-shaped	Omnidirectional	-21 dB	-25 dB

mode and dual band-notch mode is depicted in Fig. 11. It can be seen that the gain falls sharply in the vicinity of 3.5 and 5.5 GHz. For other frequencies outside the notch-band, the antenna exhibits stable gain performance. The simulated efficiency in the UWB band is more than 89%, while that of the notch-band sharply decreases to 36%.

Finally, Table 3 compares the proposed and other reported antennas with reconfigurable band-notch characteristics. Compared to the antennas with reconfigurable single band-notch property [7,11,12], the antenna in this work has single and dual band-notch functions. Also, the size of the proposed antenna is the smallest among the single and dual band-notch antennas [8-10,13].

Table 3. Performance of antennas with reconfigurable band-notch characteristics

Antenna	Size (mm ³)	RF switch	Switch number	Notch-bands	Relative dimensions
Ref. [7]	20 × 20 × 0.8	PIN diode	1	Single	0.34λ ₁ × 0.34λ ₁
Ref. [8]	45 × 40 × 1.6	PIN diode	3	Single/dual	0.74λ ₁ × 0.66λ ₁
Ref. [9]	24.8 × 30.3 × 0.8	PIN diode	3	Single/dual	0.33λ ₁ × 0.40λ ₁
Ref. [10]	32 × 27 × 1.6	PIN diode	3	Single/dual	0.47λ ₁ × 0.40λ ₁
Ref. [11]	30 × 30 × 0.8	Varactor	1	Single	0.44λ ₁ × 0.44λ ₁
Ref. [12]	25 × 25 × 0.8	Photoconductive switch	5	Single	0.29λ ₁ × 0.29λ ₁
Ref. [13]	45 × 30 × 1.5	Silicon dice	2	Single/dual	0.65λ ₁ × 0.44λ ₁
Proposed	31 × 18 × 0.8	PIN diode	2	Single/dual	0.47λ ₁ × 0.27λ ₁

Conclusion

A compact UWB monopole antenna with reconfigurable band-notch characteristics is proposed. The band-notch performance in the WiMAX and WLAN bands is realized by etching an open-ended slot on the radiating patch and an inverted U-shaped slot on the ground plane, respectively. By controlling the states of the PIN diodes embedded in the slots, the antenna can switch between a UWB mode, two single band-notch modes, and a dual band-notch mode. Also, the antenna exhibits good radiation patterns and stable gain except for the notch-bands.

Acknowledgements. This work was supported by the National Science Foundation of China (61771295, 61172045) and the Shanxi “1331 Project” Key Subjects Construction (1331KSC).

References

- Mehranpour M, Nourinia J, Ghobadi C and Ojaroudi M (2011) Dual band-notched square monopole antenna for ultrawideband applications. *IEEE Antennas and Wireless Propagation Letters* **11**, 172-175.
- Yadav S, Gautam AK, Kanaujia BK and Rambabu K (2016) Design of band-rejected UWB planar antenna with integrated bluetooth band. *IET Microwaves, Antennas & Propagation* **10**, 1528-1533.
- Liu JJ, Esselle KP, Hay SG and Zhong SS (2013) Planar ultra-wideband antenna with five notched stop bands. *Electronics Letters* **49**, 579-580.
- Wang JH, Yin YZ and Liu XL (2014) Triple band-notched ultra-wideband antenna using a pair of novel symmetrical resonators. *IET Microwaves, Antennas & Propagation* **8**, 1154-1160.
- Ojaroudi M and Ojaroudi N (2014) Ultra-wideband small rectangular slot antenna with variable band-stop function. *IEEE Transactions on Antennas and Propagation* **62**, 490-494.
- Peng L, Wen BJ, Li XF, Jiang X and Li SM (2016) CPW fed UWB antenna by EBG with wide rectangular notched-band. *IEEE Access* **4**, 9545-9552.
- Valizade A, Ghobadi C, Nourinia J and Ojaroudi M (2012) A novel design of reconfigurable slot antenna with switchable band notch and multiresonance functions for UWB applications. *IEEE Antennas and Wireless Propagation Letters* **11**, 1166-1169.
- Kalteh AA, DadashZadeh GR, Naser-Moghadasi M and Virdee BS (2014) Ultra-wideband circular slot antenna with reconfigurable notch band function. *IET Microwaves, Antennas & Propagation* **6**, 108-112.
- Oraizi H and Shahmirzadi NV (2017) Frequency- and time-domain analysis of a novel UWB reconfigurable microstrip slot antenna with switchable notched bands. *IET Microwaves, Antennas & Propagation* **8**, 1127-1132.
- Srivastava G, Dwari S and Kanaujia BK (2015) A compact UWB antenna with reconfigurable dual notch bands. *Microwave and Optical Technology Letters* **57**, 2737-2742.

11. **Aghdam SA** (2014) A novel UWB monopole antenna with tunable notched behavior using varactor diode. *IEEE Antennas and Wireless Propagation Letters* **13**, 1243–1246.
12. **Zheng SH, Liu XY and Tentzeris MM** (2014) Optically controlled reconfigurable band-notched UWB antenna for cognitive radio systems. *Electronics Letters* **50**, 1502–1504.
13. **Zhao DS, Lan LT, Han YF, Liang F, Zhang QL and Wang BZ** (2014) Optically controlled reconfigurable band-notched UWB antenna for cognitive radio applications. *IEEE Photonics Technology Letters* **26**, 2173–2176.
14. **Rumsey VH** (1966) *Frequency Independent Antennas*. New York: Academic Press.
15. **Huang CY and Su JY** (2011) A printed band-notched UWB antenna using quasi-self-complementary structure. *IEEE Antennas and Wireless Propagation Letters* **10**, 1151–1153.



Liping Han received the B.S., M.S., and Ph.D. degrees in electronic engineering from Shanxi University, Taiyuan, China, in 1993, 2002, and 2010, respectively. Currently, she is an Associate Professor with the School of Physics and Electronic Engineering, Shanxi University. Her research interests include microwave and millimeter-wave integrated circuits and microstrip antenna.



Jing Chen received the B.S. degree in electronic science and technology from Jiangsu Normal University, Xuzhou, China in 2016. Currently, she is a graduate of Shanxi University, Taiyuan, China. Her research interests include design and analysis of reconfigurable antenna.



Wenmei Zhang received the B.S. and M.S. degrees in electronic engineering from Nanjing University of Science and Technology, Nanjing, China, in 1992 and 1995, respectively, and the Ph.D. degree in electronic engineering from Shanghai Jiao Tong University, Shanghai, China, in 2004. Currently, she is a professor with the School of Physics and Electronic Engineering, Shanxi University, Taiyuan, China. Her research interests include microwave and millimeter-wave integrated circuits, EMC, and microstrip antenna.